Final Scientific/Technical Report

Project Title
Geophysical Signatures of Crack Network Coalescence in Rocks at Multiple Length Scales

Award Number
DE-SC0019117

Project Period
09/01/2018- 08/31/2024

Recipient Institution
Colorado School of Mines

Principal Investigator
Ahmadreza Hedayat, Ph.D.

Contact Information
(303) 273-3401; hedayat@mines.edu

Business Mailing Address of the Principal Investigator
1500 Illinois St, Golden, Colorado 80401

DOE/Office of Science Program Office
Basic Energy Sciences- Geoscience Program

Acknowledgment: This research work was sponsored by the U.S. Department of Energy, Office of Basic Energy Sciences, Geosciences program under Award Number DE-SC0019117. This support is gratefully acknowledged.

Table of Content

1. Executive Summary

The main goal of the research project was to identify the geophysical signatures of fracture growth in natural rocks by utilizing novel geophysical techniques. The research objectives were to (a) investigate the potential for geophysical methods to determine when cracks initiate, the types and locations of propagated cracks, and the coalescence of networks of cracks in natural rocks at multiple scales, (b) determine how damage at the microscale evolved into damage at the macroscale and then link the microscopic and macroscopic observations, (c) quantify crack coalescence in rocks under realistic stress conditions using coupled mechanical-geophysical-optical visualization, and (d) identify the precursors in geophysical signals to crack coalescence. The following research thrusts were explored to achieve the research objectives: (1) uniaxial compression testing of rock specimens with and without a set of pre-existing flaws and (2) triaxial compression testing of natural rock specimens. These thrusts allowed for exploring fracturing in rocks under realistic in situ environments and at multiple scales. This project provided educational opportunities for nine graduate and undergraduate students and resulted in 27 peer-reviewed publications.

This first research thrust focused on investigating the micromechanics of fractures in rocks through uniaxial compression testing combined with advanced geophysical and imaging techniques, specifically acoustic emission (AE) monitoring, ultrasonic imaging, and 2-dimensional Digital Image Correlation (2D-DIC). By examining damage processes under time-independent and time-dependent loading conditions, insights into damage localization, crack initiation, and fracturing mechanisms were gained. It was observed that the AE signals and the strain-based measurements directly reflect the state of damage in the rock specimen and could be used to identify the cracking levels, such as the crack initiation (CI) and crack damage (CD), and the mode of deformation. A novel calibration apparatus was developed to enhance the accuracy of AE sensors, allowing for the estimation of key parameters such as magnitude, source dimension, stress drop, and radiated seismic energy associated with the fractures. The findings highlighted significant variations in the temporal evolution of AE source parameters during the primary, secondary, and tertiary stages of creep, identifying tensile cracking as the primary deformation mode.

The second research thrust focused on enhancing the understanding of fracturing processes in natural rocks through triaxial compression testing, real-time AE monitoring, and ultrasonic monitoring. We investigated the impact of various factors such as fracture propagation regimes, injection parameters, rock types, and pre-existing conditions on the hydraulic fracture (HF) behavior using scaled true-triaxially loaded specimens of Barre granite and Lyons sandstone. Custom sensor housing facilitated concurrent active and passive monitoring to analyze hydro-mechanical responses and microseismicity associated with different HF scenarios. A coupled investigation of passive microseismicity and active signal attributes permitted a detailed comprehension of the various HF processes (aseismic deformation, fracture initiation and propagation, fluid permeation, and leak-off) and their dependence on the specific rock type. The findings of this research demonstrated the effectiveness of AE monitoring techniques in providing valuable insights into the impact of various factors on the behavior and dynamics of HF processes. The advancements in monitoring techniques, offering a more thorough and precise approach, represent a significant step towards optimizing HF practices and ensuring sustainable resource extraction.

2. Acknowledgments

This research work was sponsored by the U.S. Department of Energy, Office of Basic Energy Sciences, Geosciences program under Award Number DE-SC0019117. This support is gratefully acknowledged. Additional support provided by the Colorado School of Mines is highly appreciated. In addition, the following individuals who collaborated on this project are gratefully acknowledged: Drs. Deepanshu Shirole, Gabriel Walton, Amin Gheibi, Sana Zafar, Awais Butt, Omid Moradian, and Bing Li.

3. Accomplishments and Objectives

The main goal of this research project was to identify the geophysical signatures of crack initiation and growth in natural rocks. Discovering the processes resulting in crack network coalescence and their accompanying geophysical signals in natural rocks were the main objectives of this research project. The original research hypothesis was that the measurement of the strain and stress fields around the tips of cracks, investigation of geophysical waveforms transmitted through and reflected off the rock materials, and analysis of the acoustic analysis data during crack coalescence experiments would allow accurate identification of the crack types and the coalescence signatures at multiple length scales. We tested this hypothesis for two specific geometries of uniaxial compression and triaxial compression, and in both scales, we identified the seismic and aseismic processes associated with fracturing and their evolution.

The actual tasks performed closely followed the proposed activities included in the approved and funded application. These proposed tasks were: (a) to conduct uniaxial compression tests on rock specimens with pre-existing flaws through concurrent optical and geophysical visualization, and (b) to conduct true-triaxial compression tests on rock specimens (analogue and/or natural) with a fracture network using concurrent active and passive geophysical imaging.

This project contributed to the quantitative analysis of the progressive damage observed in rocks under monotonic and time-dependent loading conditions by the application of AE monitoring, ultrasonic imaging, and image-based strain analysis approaches. The strain metrics extracted from the image-based strain profiles facilitated the real-time analysis of tensile and shear damage evolution in the rock volume. This analysis was then utilized to establish a quantitative correlation between the acoustic-visual observation of grain-scale microcrack accumulation in brittle rocks. A source parameter estimation methodology was developed, utilizing calibrated piezoelectric sensors, for the seismic characterization of the fractures produced during time-dependent stress relaxation and creep experiments. Fracture mechanisms associated with rock damage were analyzed, and their effect on the fracture parameters, such as size, seismic moment, moment magnitude, stress drop, and radiated seismic energy, was estimated. The energy budgeting approach was utilized to estimate the different energy components and associated radiation efficiencies for stress relaxation and creep experiments. It was observed that radiation efficiency in case of creep was higher than stress relaxation.

The research project contributed towards advancing the understanding of the complex HF phenomena in rocks by the application of geophysical acoustic techniques. By selecting/controlling different parameters or boundary conditions, this research investigated their

effects on the corresponding HF behavior through detailed seismic investigations. The selection of appropriate parameters might be representative of specific scenarios encountered during field HF operations. The findings of this research, when applied effectively, can contribute substantially to improving the understanding, control, and optimization of HF stimulation operations in the field. The distinct scientific contributions of this research project in enhancing the understanding of HF and the associated fracturing processes are detailed as follows:

For the first time, various classification criteria were employed to determine the fracture source mechanisms and their evolution for the microseismicity detected during scaled laboratory HF experiments. This research project established that the choice of classification criteria would significantly impact the determined proportions of fracture source mechanisms. This finding enhances our laboratory HF experiments, providing valuable insights for future research and field applications.

A major contribution of this research was conducting seismic energy budgeting for scaled laboratory HF experiments, including determining seismic source parameters and comparing them to large-scale induced earthquakes. This was achieved by conducting an absolute calibration of the passive AE sensors using a calibration station configured exactly like the settings of the laboratory HF experiments. Perhaps it is the only study that has explored the scale invariability of seismic source parameters between lab-scale HF microseismic events and field-scale induced earthquakes.

It was demonstrated successfully that active and passive seismic monitoring techniques can be employed in conjunction during laboratory HF experiments. A methodology was proposed to eliminate the active monitoring contamination from passive microseismicity data, enabling a novel joint investigation of active signals' attributes and passive microseismicity. This allowed the assessment of their variable sensitivities to various aseismic and seismic HF processes in granitic rocks. Overall, the research provided a valuable methodological framework for integrating active and passive seismic monitoring in laboratory HF studies, enhancing our comprehension of the HF processes. This type of monitoring has significant potential for characterizing seismic and aseismic damages occurring in brittle materials such as rocks and concrete.

The comparative analysis of HF behavior in granite and sandstone using simultaneous active and passive seismic monitoring techniques provided valuable insights into the differences in HF initiation and propagation, seismic response, and overall fracturing processes between these two rock types. This was accomplished by thoroughly investigating the relationship between the attributes of active signals and passive microseismicity across various rock types. This analysis enhanced our understanding of the factors and processes influencing HF behavior in granite and sandstone, contributing to developing more effective stimulation techniques in diverse geological settings.

The effect of pre-existing fracturing on the HF patterns was analyzed in terms of hydro-mechanical response, morphology, fracture source mechanisms, variations in seismic source parameters, and radiated seismic energy. This was accomplished by inducing different levels of fracturing in granite blocks before conducting the HF experiments. These findings provided insights into the HF behavior of fractured rock masses encountered in the field, advancing our understanding of the effects of different levels of pre-existing fractures/discontinuities on the HF processes.

4. Project Activities

To minimize duplication, this final technical report includes citations of all peer-reviewed publications from this project. Thirteen journal papers and fourteen conference proceedings have been published. To make all publications publicly available, they have been submitted through annual progress reports or uploaded directly to the DOE Office of Scientific and Technical Information (OSTI) website. The following provides some selected and notable research highlights.

Highlight 1. Evolution of tensile and shear cracking under compression

We performed laboratory-scale unconfined compression experiments on Barre granite specimens with pre-existing flaws to study the evolution of tensile and shear cracking that occurs during different stress levels (Figure 1). Moment tensor inversion of AE events in combination with the non-elastic strain component obtained through the 2D-DIC technique was used to track the changes in the source mechanisms of the stress-induced cracks. The mode of deformation computed from the image-based strain profiles enabled visual comparison of the nucleation, growth, and interaction of the tensile and shear cracks with the microseismic source mechanism observed by moment tensor inversion of the AE events. Comparing the results obtained from the two techniques on the same dataset demonstrated a quantitative correlation between the acoustic and visual observations in terms of the cracking mechanisms obtained at different stages of cracking from crack initiation at the flaw tips to the failure of the rock specimen (Figures 2-3) (Zafar et al. 2022a).

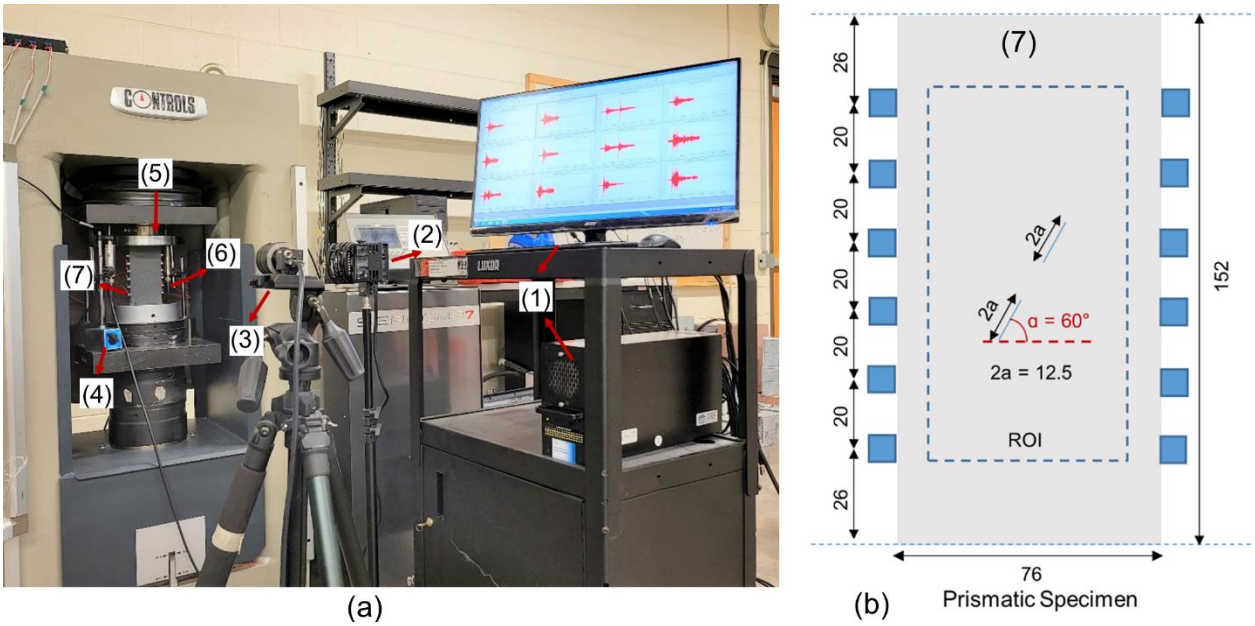

Figure 1. Experimental setup for AE monitoring and 2D-DIC procedures: (a) (1) AE monitoring system, (2) lighting system for DIC, (3) CCD camera, (4) Linear variable differential transformer (LVDT), (5) Load cell, (6) Nano 30 AE sensors, (7) Barre granite specimen; (b) Speckled Barre granite specimen, small boxes denote the position of the AE transducers, the dotted line represents the ROI, flaw length is 12.5 mm and flaw inclination angle is 60° (all the dimensions are in mm) (After Zafar et al. 2022a).

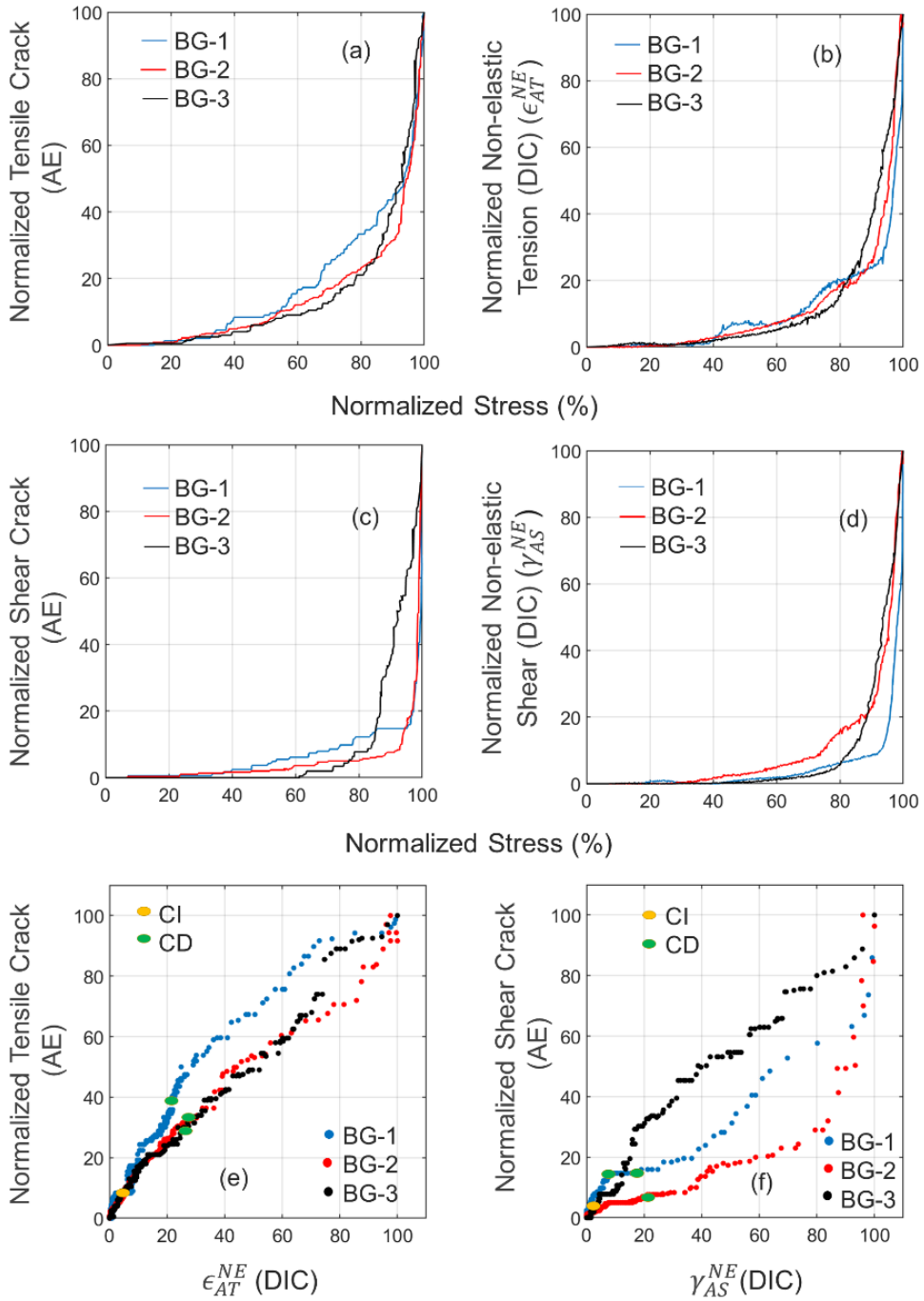

Figure 2. (a) Variation of tensile crack evolution obtained through AE in the region of interest (ROI) for all the three Barre granite (BG) specimens; (b) Variation of non-elastic component of tensile strain obtained through DIC for the three specimens in the ROI; (c) Variation of shear crack evolution obtained through AE; (d) Variation of non-elastic component of maximum shear strain obtained through DIC in the ROI; (e) Correlation between the tensile crack evolution and the non-elastic tensile strain component in the ROI for the three rock specimens (blue- BG-1, red-BG-2, black-BG-3), (f) Correlation between the shear crack evolution and the non-elastic maximum shear strain component in the ROI for the three rock specimens (blue-BG-1, red-BG-2, black-BG-3), the CI and CD has been distinguished by the yellow and green circles on the map (After Zafar et al. 2022a).

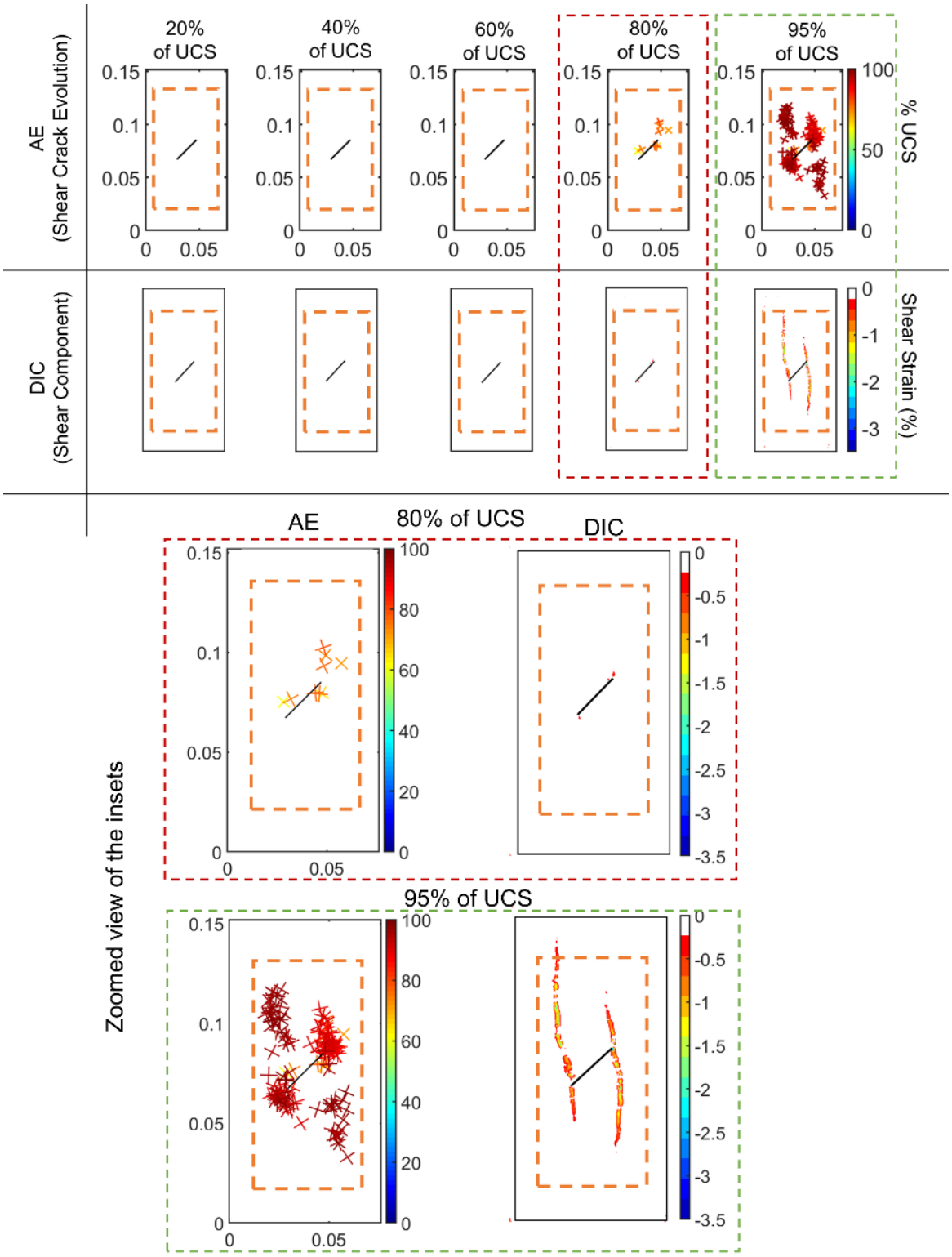

Figure 3. Comparison between the mode of deformation obtained through AE (shear cracks) and DIC (shear component of strain) at different stress levels in the ROI for BG-3, insets show the zoomed view of the subfigures at 80% and 95% of the UCS (After Zafar et al. 2022a).

Highlight 2. Micromechanics of fracture propagation during relaxation and creep

Time-dependent rock deformation caused by the initiation and growth of fractures leads to the weakening of the rock mass. Understanding the fracturing mechanisms involved in time-dependent behavior in brittle rocks is very important. To achieve this goal, a systematic series of experiments was performed on double-flawed prismatic Barre granite specimens under unconfined compression. The first series aimed to identify the failure mechanism in the short-term failure mode under monotonic loading. The second series involved multistage relaxation (constant strain) experiments to analyze the damage at different strain levels, and the third series explored fracture propagation under multistage creep (constant load) experiments. The spatial and temporal evolution of cracking mechanisms were evaluated using the AE and 2D-DIC techniques to observe the whole crack growth process as well as the accumulated inelastic strain at the specified region of interest. Results suggest that in the case of multistage creep experiments, the time to failure was less compared to the multistage relaxation when loaded above the crack damage threshold (CD) estimated from the monotonic testing. The frequency magnitude distribution of the AE events generated in the three loading conditions followed the Gutenberg Richter model. A relatively lower b-value was obtained for the creep experiments, indicative of high-energy AE events and faster crack growth. In addition, the AE and DIC results also revealed a high evolution of tensile cracks at different stages of creep and relaxation compared to shear and mixed-mode cracks (Figure 4) (Zafar et al. 2022b).

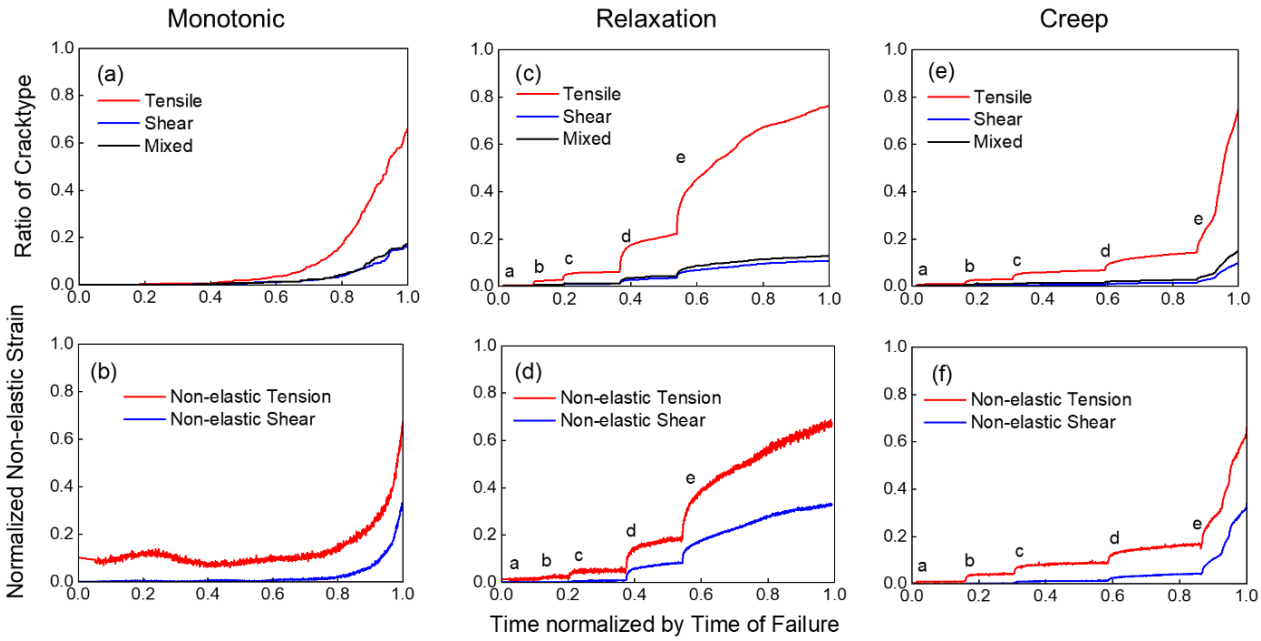

Figure 4. Temporal evolution of different types of cracks for monotonic loading experiment obtained through (a) moment tensor inversion; (b) DIC analysis; for the relaxation experiments obtained through (c) moment tensor inversion; (d) DIC analysis; for the multistage creep experiments through (e) moment tensor inversion; (f) DIC analysis (After Zafar et al. 2022b).

Highlight 3. Energy budget of brittle fracturing in granite

Creep and relaxation are the two major time-dependent fracturing processes in rocks. While a considerable amount of research has been done in understanding these two mechanisms, critical gaps remain regarding how different energy components evolve during time-dependent fracturing processes in rocks. A series of relaxation and creep experiments were conducted on prismatic Barre granite specimens in the laboratory to estimate the energy budget of brittle fracturing in granite. For the input energy the work done by the machine (W) is calculated and for the output energy the radiated seismic energy (E_R), released in the form of AEs, is calculated as the only measurable output energy component in the conducted experiments. The low-frequency plateau (Ω_0) and corner frequency (f_0) for each AE waveform was estimated by fitting the observed AE spectra with the theoretical spectra using Omega model. These parameters were used to estimate the seismic moments (M_0) based on the radiation pattern for the double couple (shear) and non-double-couple (non-shear) events. The range of f_0 and M_0 varied from 150 kHz to 750 kHz and 10^{-4} to 10^{-1} N.m, respectively (Figure 5). Moment magnitude (M_w) varied in a wider range from -9 to -6 in creep and -8.5 to -7 in relaxation. Stress drops ($\Delta\sigma$) and source radius (r) were estimated for the AEs using Brune's model. The results report on three primary observations: (1) the effects of different source mechanisms on the estimated source parameters showed that M_0 and $\Delta\sigma$ were higher for double-couple (DC) events as compared to non-double-couple (NDC) events in both relaxation and creep. (2) The seismic efficiency in the case of creep is 70% higher than that in relaxation. (3) The stress drop estimated in relaxation and creep demonstrated a breakdown in scaling with the seismic moment (Figure 6) (Zafar et al. 2023).

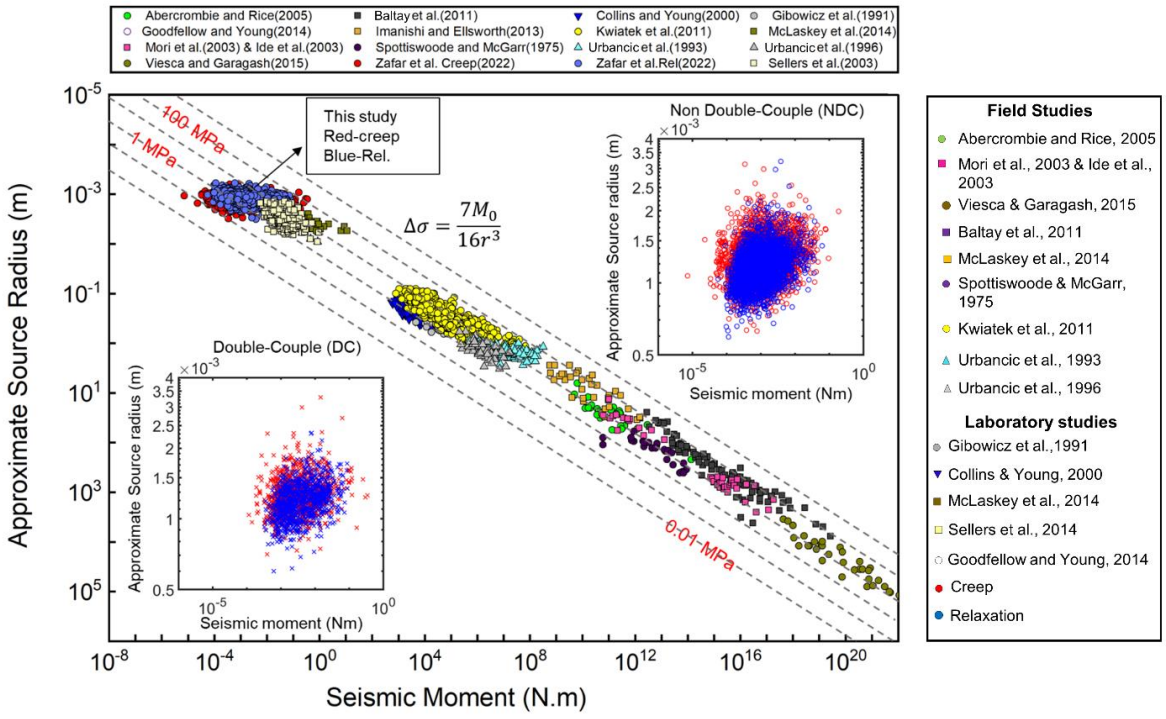

Figure 5. Comparison of our laboratory source estimates of approximate source radius and seismic moment for relaxation and creep to those from a range of other studies (considering each study calculated the source radius and seismic moment using different seismological models) (After Zafar et al. 2023).

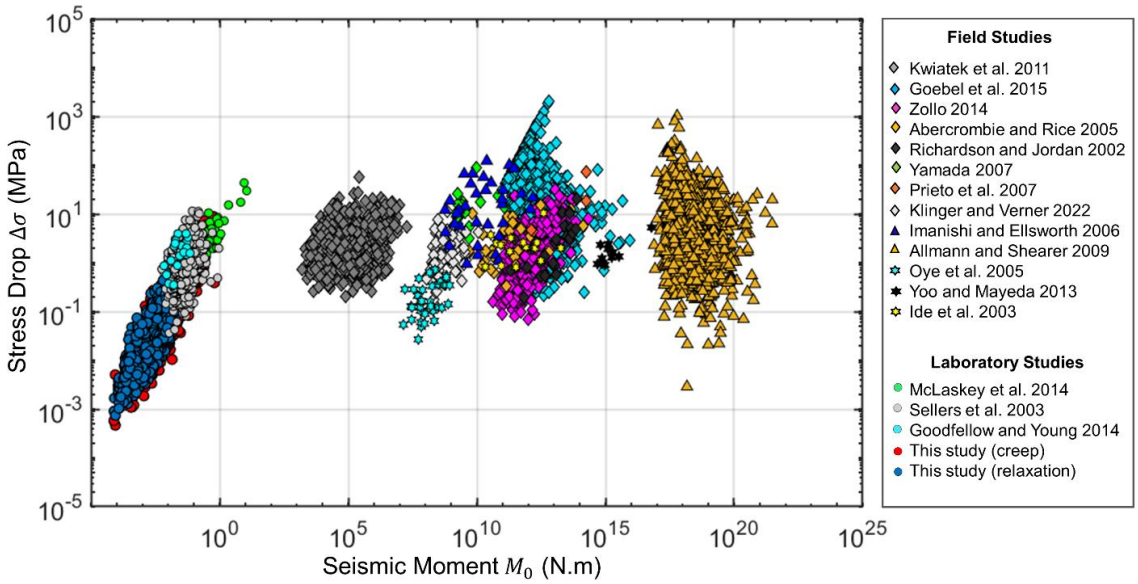

Figure 6. Stress drop scaling with seismic moment for field and laboratory studies. The red and blue circles represent the observations made in the current stud. Field and other lab data collected from Cocco et al. (2016) (After Zafar et al. 2023).

Highlight 4. Brittle creep and associated acoustic emissions in granite

Results from conventional creep experiments show that three stages of creep (trimodal creep curve) exist for brittle materials. The first stage is the primary stage where the strain rate is inversely proportional to time. In the secondary stage, partially reversible strain occurs in which the strain rate is small and constant. The final stage is the tertiary stage, where an accelerated strain rate occurs, causing the rock to fail. It is hypothesized that AE can be used as a proxy to identify the transitions from one stage to another in creep; therefore, the different focal mechanisms of the fractures produced and the associated seismic source parameters in the three stages of creep in brittle rocks are worthy of systematic exploration. Our research work aimed at investigating how AE signatures can monitor brittle deformations during the three stages of creep and its correlation with the mechanical observations so that these AE signatures can be relied upon to reveal critical creep stages and the impending failure at the field scale. Creep experiments were conducted on double-flawed prismatic Barre granite specimens in the laboratory under uniaxial compression to investigate the temporal and spatial evolution of the AE events during the primary, secondary, and tertiary stages of creep (Figure 7). Results illustrate that the creep in granite follows Omori's law and inverse Omori's law in the primary and tertiary creep regimes, respectively. Non-double-couple (NDC) sources were the dominant failure mechanisms in all stages of creep. These results can be of great importance as continuous and non-destructive monitoring of structures in rock and the associated seismicity can serve as precursory indications of instability of the rock engineering structures and in the analysis of earthquake aftershocks and recurrences.

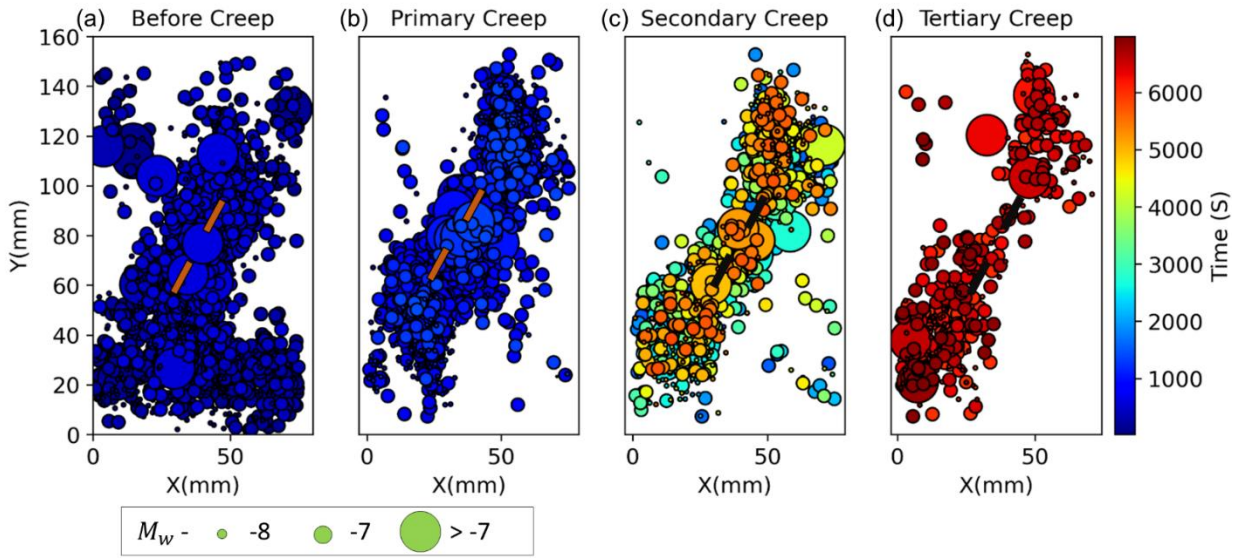

Figure 7. Spatial evolution of the AE sources and their moment magnitudes (Mw at various stages of loading and creep; (a) Before creep; (b) Primary Creep; (c) Secondary Creep; (d) Tertiary Creep.

Highlight 5. Microseismic monitoring of laboratory hydraulic fracturing experiments

While HF is a widely employed process, the underlying fracturing processes are still heavily contested. The attributes of the HF-generated fracture network can exhibit substantial variation when dealing with specific HF propagation regimes encountered in the field. In this research project, HF experiments were performed on true-triaxially loaded Barre granite cubes, with microseismic monitoring, to identify and characterize the fracturing mechanisms associated with different viscosity injection fluids (Figure 8). Utilizing fluids with high (oil/1450 cP) and low (water/1 cP) viscosity represented two key HF propagation regimes: viscosity- and toughness-dominated. The experiments conducted with oil involved higher breakdown pressures, larger fluid volumes, and slower fracture propagation speeds. The frequency-magnitude distribution (b-value) for all experiments (1.9-2.3) was similar to those encountered for large-scale operations. Slightly larger b-values were encountered during the initiation phase (2.4-2.7) relative to the fracture propagation and post-fracturing phases (1.9-2.2). Polarity and moment-tensor inversion were used to characterize the source mechanisms. For the HF experiments with oil, tensile fractures were most dominant (92%) in the initiation phase compared to fracture propagation and post-fracturing phases (70-75%) (Figure 9). Similar tensile fracturing dominancy was not observed with water, which is attributable to fluid permeation and leak-off. Regardless of the injection fluid or classification criteria employed, tensile fractures were the dominant type consistently, with fewer occurring in water experiments, but the specific ratio of crack types varied with different source mechanism criteria employed (Butt et al. 2023a).

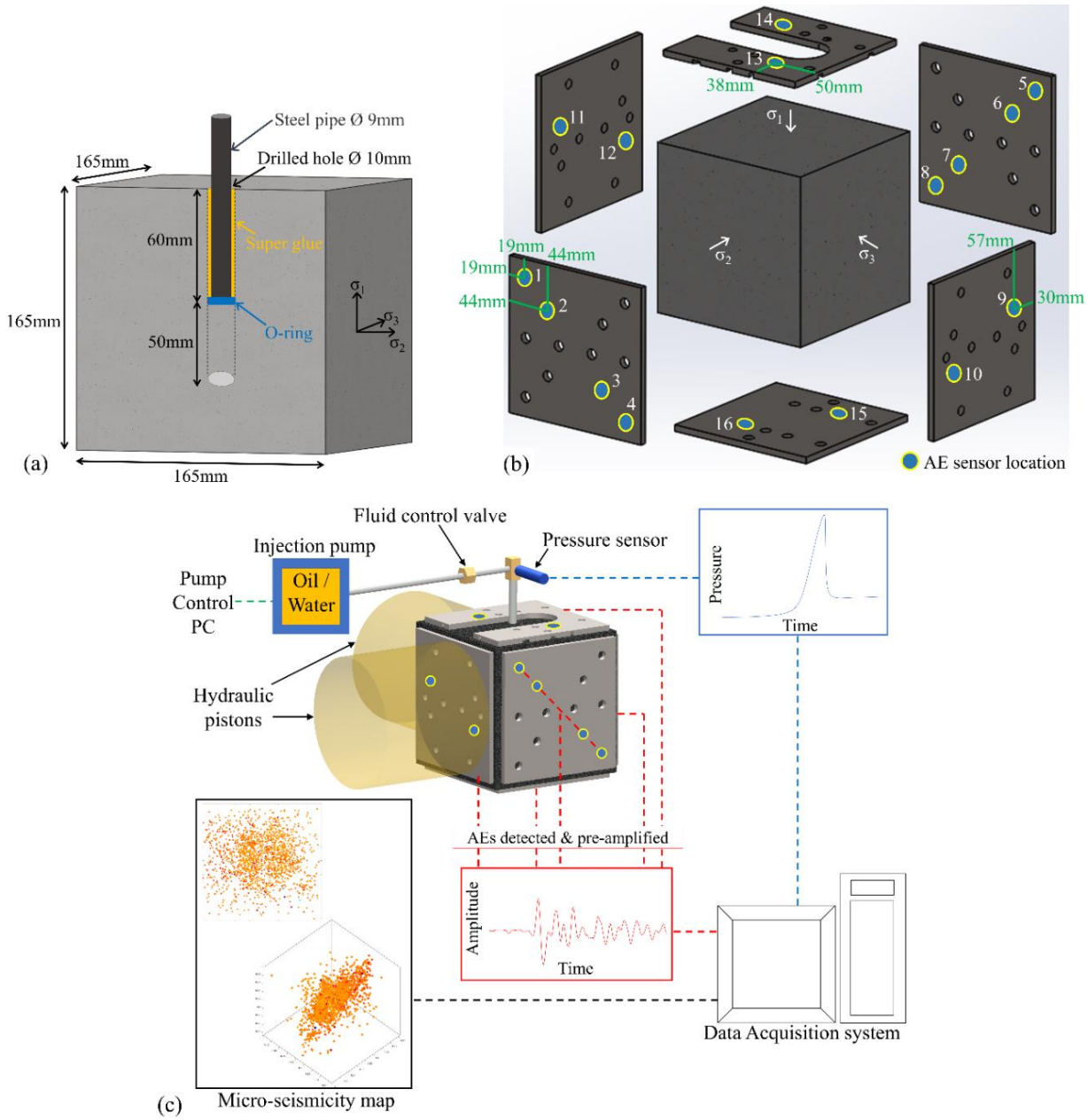

Figure 8. (a) Schematic of the specimen and borehole configuration used for the HF experiments. A small borehole with a radius of 5 mm was drilled with respect to its distance to the boundaries of the cubic block (82.55 mm) (b) The location of 16 Nano-30 AE sensors in different platens, selected for the HF experiments providing sufficient coverage of the entire block. (c) Schematic of the complete experimental setup. The data from the AE sensors were amplified and recorded in the computer for post-experiment analysis. The data from the hydraulic pistons and the pressure sensor, located 50mm above the borehole entrance, was also recorded in the same computer to achieve synchronization between the pressure, confining stress, and the AE data (not to scale) (After Butt et al. 2023a).

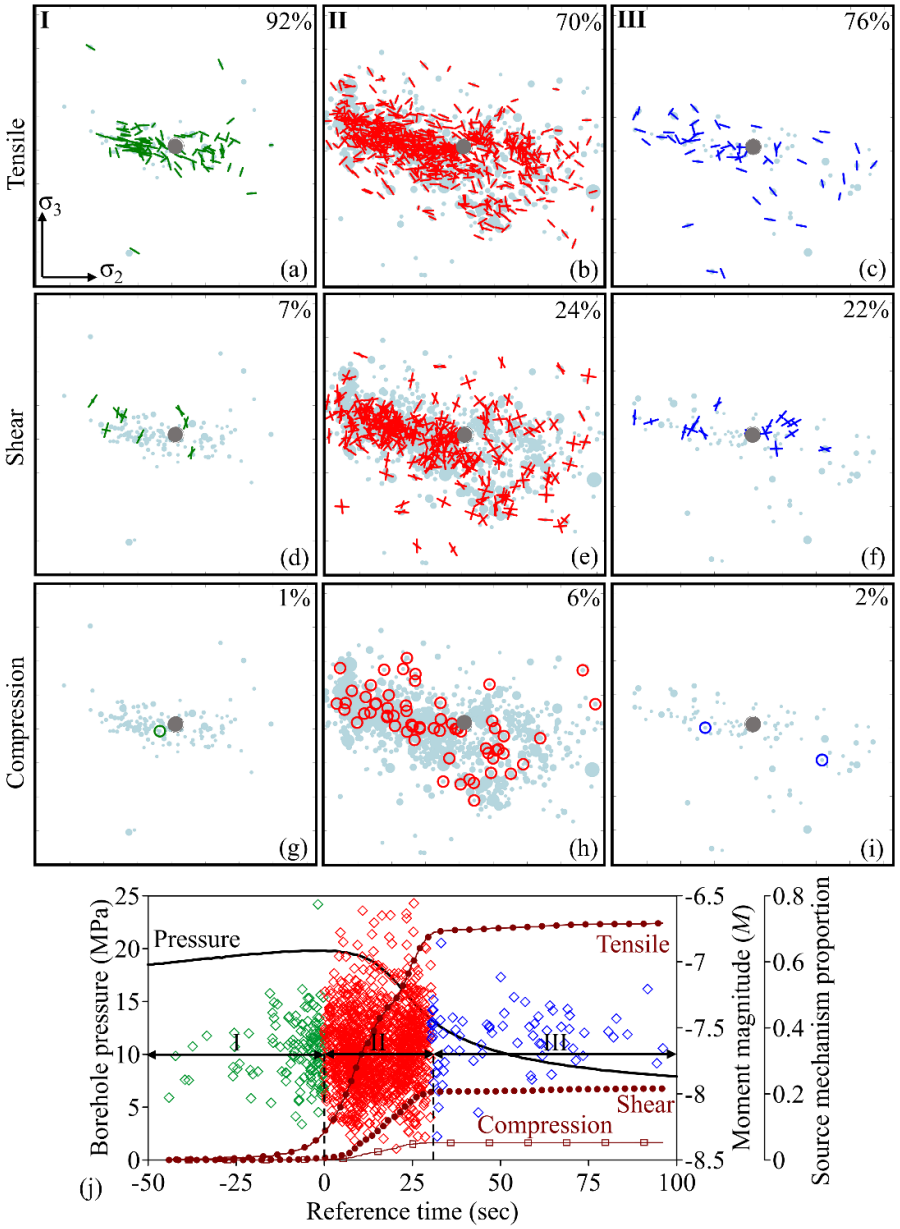

Figure 9. The evolution of crack source mechanisms during the three phases of Oil_Test#1 experiment, determined based on the ISO-CLVD method: tensile (a-c), shear (d-f), and compression (g-i) mode, along with the percentages, in the top, middle and bottom rows respectively. The color of the symbols corresponds to the fracturing phase. In (j), symbols represent the evolution of moment magnitude in different phases of the experiment. The dark red color lines indicate the evolution of source mechanism proportion (tensile, shear, and compression) (After Butt et al. 2023a).

Highlight 6. Energy budgeting of laboratory hydraulic fracturing

We investigated the source parameters of microseismicity detected during laboratory HF of granite conducted with high- (gear oil/1000 cP) and low- (water/1 cP) viscosity injection fluids. These HF experiments were monitored with a real-time acoustic emission (AE) setup consisting of 16 calibrated sensors. The spectral parameters (corner-frequency and low-frequency spectral plateau) were determined for each AE event by fitting Omega-models with variable high-frequency fall-

off exponents to the detected AE signals. Seismic parameters such as seismic moment, source radius, stress drop, and seismic energy were determined after incorporating the focal-mechanism information determined through moment-tensor inversion. Higher breakdown pressures and fracture propagation times, along with greater number and strength of microseismicity, were observed for experiments conducted with higher-viscosity fluid (Figure 10). For both experiments, an inverse relationship was observed between corner frequency and seismic moment, similar to those observed for large-scale induced earthquakes. The corner frequency, seismic moment, stress drop, and seismic energy were noticeably higher for the higher-viscosity injection fluid. However, the seismic source radius was slightly larger for the lower-viscosity fluid. Varied spectral and seismic parameters (16-29%) were determined based on the adopted Omega model; however, these variations did not affect the observed relationships between seismic parameters in high- and low-viscosity experiments. The seismic efficiency was <<1% (10^{-6} - 10^{-4} %) for both experiments, but it was much lower for experiments conducted with lower-viscosity injection fluid, implying a more aseismic response. Comparing the seismic source parameters determined in this research project with those derived from large-scale induced earthquakes suggests potentially similar scaling relationships.

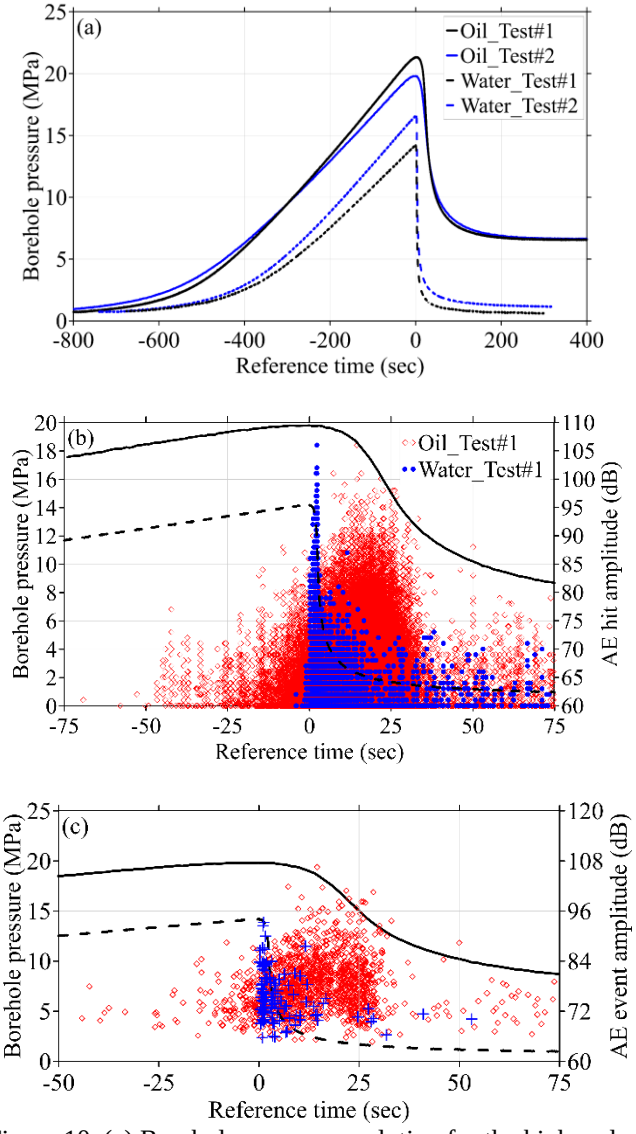

Figure 10. (a) Borehole pressure evolution for the high and low viscosity HF experiments (b) Evolution of pressure and AE hits for a selected duration of reference time (±75) for one HF experiment each with high and low viscosity fluids (a) Borehole pressure and determined AE events for the high and low viscosity HF experiments.

Highlight 7. Laboratory investigation of fracturing using active and passive seismic monitoring

Active and passive seismic monitoring techniques have been employed in the field mainly for tracking or mapping the propagating hydraulic fracture. Although both these monitoring techniques provide valuable information about the generated fracture network, it is difficult for either technique to comprehensibly identify the different processes associated with HF. The combined active and passive monitoring has the potential for better characterization of complex HF phenomena. In this research project, laboratory HF experiments with

combined active and passive seismic monitoring were conducted on true triaxially loaded Barre granite cubes with different fluid injection rates. The seismic inelastic fracturing was detected by 10 passive acoustic emission sensors, where 3678 and 2370 seismic source events were detected for the high and low injection rate experiments, respectively. For active monitoring, strong variations in the attributes of signals were observed which were transmitted through four source-receiver pairs, placed both perpendicular and parallel to the generated hydraulic fracture. Positive velocity changes were observed for active sensor pairs with ray paths passing through the generated hydraulic fracture, indicating fluid permeation. In contrast, a slight but permanent velocity decrease was characterized by isolated dry deformation. Compared to velocity, the energy of the active signals was 1-2 orders of magnitude more sensitive to different HF processes. However, the sensitivity and signatures of the active signal attributes were found to be dependent on the frequency range and direction of the rayath with respect to the location of the generated fracture network. Using the coupled evaluation of the active and passive signals, we were able to systematically identify various HF processes, including I) aseismic deformation, II) fracture initiation and fluid permeation, III) pressure buildup, IV) fracture propagation, and V) pressure release and leak-off (Figure 11). The results of this project showed that combining the respective advantages of active and passive seismic techniques and using both of them to monitor the failure processes can facilitate a more comprehensive understanding and better control of the hydraulic stimulations in subsurface operations (Butt et al. 2023b).

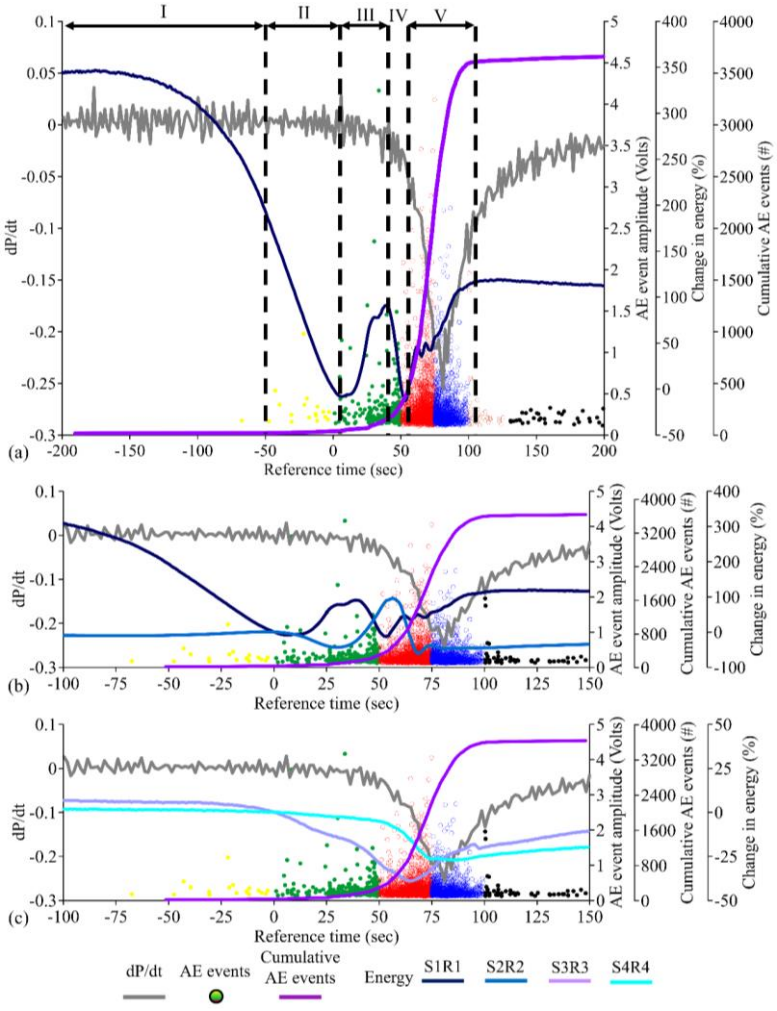

Figure 11. Pressurization rate ($\frac{dP}{dt}$), AE events, cumulative AE events, along with the evolution of energy of the active signals for the 0.1 ml/min HF experiment: (a) S1R1 only, for the identification of different HF processes (b) S1R1 and S2R2; perpendicular to the generated HF, and (c) S3R3 and S4R4; parallel to the generated HF (After Butt et al. 2023b).

Highlight 8. Hydraulic fracturing and seismic response of granite and sandstone

Through active and passive monitoring, we investigated the HF response of crystalline (granite) and sedimentary (sandstone) rocks.

Passive monitoring successfully mapped the generated HF, which was found to be more tortuous for granite together with a relatively higher number of microseismic events. The analysis of crack source mechanisms through moment-tensor inversion indicated a slightly lower proportion of opening cracks for granite. The sensitivity of the active signals' attributes (velocity, amplitude, and energy) was significantly higher for the granite HF processes than for sandstone (Figure 12). A combined investigation of active and signals made it possible to identify and differentiate between various HF phenomena in granite and sandstone. The initial aseismic deformation and fluid leak-off were notably prominent in granite specimens. While encountered for both granite and sandstone, stronger isolated dry fracturing induced variations in both velocity and amplitude of the active signals during granite HF. Acquiring in-depth knowledge about the specific features of induced HF in different rock types can contribute towards improved control and efficiency of stimulation operations in geologically diverse environments.

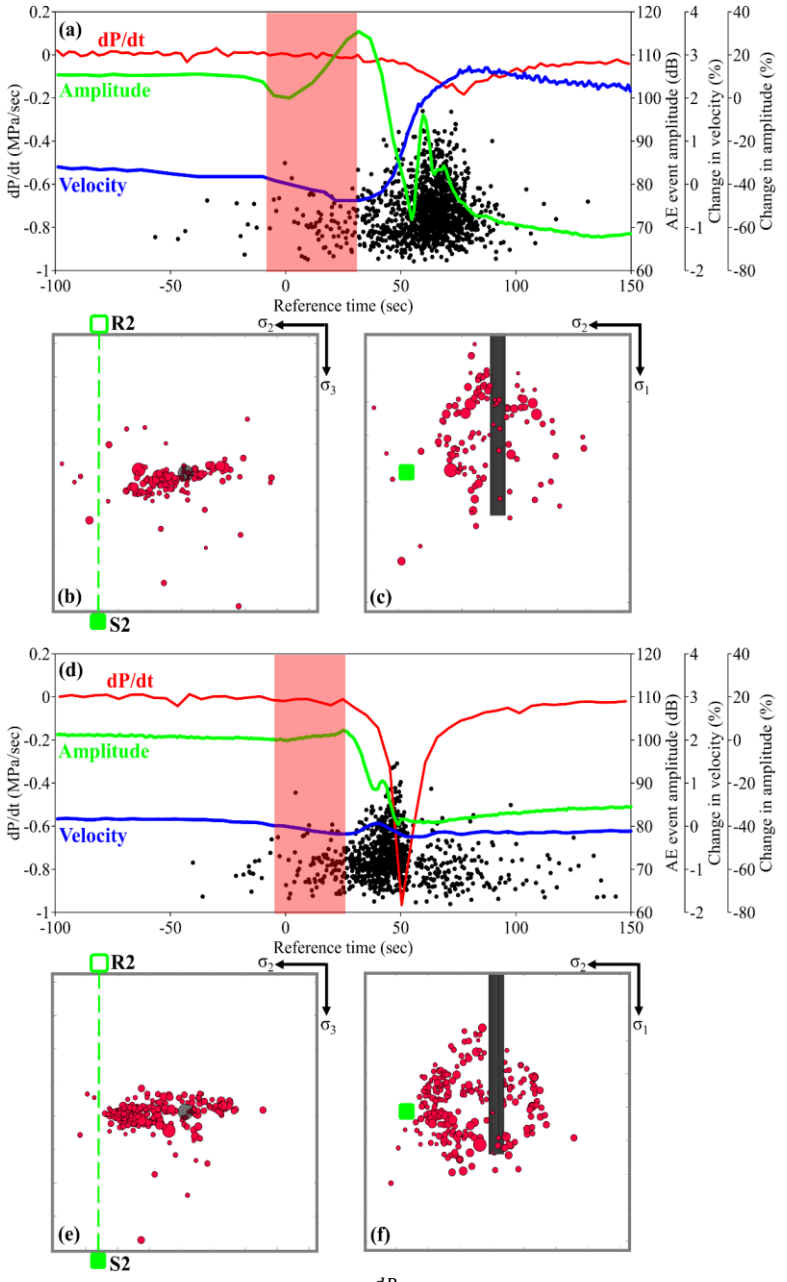

Figure 12. The pressurization rate ($\frac{dP}{dt}$) (red line) along with the change in velocity (blue line) and amplitude (green line) for the active sensor pair S2R2 during (a) granite and (d) sandstone HF experiments. The spatial distribution of AE events (red circles circles) detected during (b-c) granite and (e-f) sandstone HF experiments between the duration highlighted in (a) and (d), respectively. The location of active sensor pair (S2R2) is also included in the figure.

5. Project Outputs

Journal Publications

1. Shirole, D., Hedayat, A., and Walton, G. (2019). Experimental relationship between ultrasonic attenuation and surface strains in prismatic rock specimens, Journal of Geophysical Research - Solid Earth, 124 (6), 5770-793. https://doi.org/10.1029/2018JB017086.
2. Shirole, D., Hedayat, A., and Walton, G. (2020). Illumination of damage in intact rock specimens by ultrasonic wave transmission and reflection. Journal of Geophysical Research-Solid Earth, 125(7), e2020JB019526. https://doi.org/10.1029/2020JB019526.
3. Gheibi, A., and Hedayat, A. (2020). Ultrasonic imaging microscale processes in quartz gouge during compression and shear. Journal of Rock Mechanics and Geotechnical Engineering. https://doi.org/10.1016/j.jrmge.2020.03.011.
4. Shirole, D., Walton, G., and Hedayat, A. (2020). Experimental investigation of multi-scale strain-field heterogeneity in rocks. International Journal of Rock Mechanics and Mining Sciences 127, 104212. https://doi.org/10.1016/j.ijrmms.2020.104212
5. Shirole, D., Hedayat, A., Walton, G. (2021). Damage monitoring in rock specimens with pre-existing flaws by non-linear ultrasonic waves and digital image correlation. International Journal of Rock Mechanics and Mining Sciences, 142, 104758. https://doi.org/10.1016/j.ijrmms.2021.104758.
6. Gheibi, A., Li, H., and Hedayat, A. (2021). Detection of seismic precursors in converted ultrasonic waves to shear failure of natural sandstone rock joints. Rock Mechanics and Rock Engineering, 54, 3611-3627. https://doi.org/10.1007/s00603-021-02507-x.
7. Zafar, S., Hedayat, A., Moradian, O. (2022a). Evolution of Tensile and Shear Cracking in Crystalline Rocks Under Compression. Theoretical and Applied Fracture Mechanics, DOI:10.1016/j.tafmec.2022.103254.
8. Zafar, S., Hedayat, A., Moradian, O. (2022b). Micromechanics of Fracture Propagation During Multistage Stress Relaxation and Creep in Brittle Rocks. Rock Mechanics and Rock Engineering, 55, 7611–7627. https://doi.org/10.1007/s00603-022-03045-w.
9. Zafar, S., Hedayat, A., Moradian, O. (2023). Energy Budget of Brittle Fracturing in Granite Under Stress Relaxation and Creep. Rock Mechanics and Rock Engineering. https://doi.org/10.1007/s00603-023-03593-9.
10. Butt, A., Hedayat, A., Moradian, O. (2023a). Laboratory investigation of hydraulic fracturing in granitic rocks using active and passive seismic monitoring. Geophysical Journal International, 234 (3), 1752-1770. https://doi.org/10.1093/gji/ggad162.

11. Butt, A., Hedayat, A. & Moradian, O. (2023b). Microseismic Monitoring of Laboratory Hydraulic Fracturing Experiments in Granitic Rocks for Different Fracture Propagation Regimes. Rock Mech Rock Eng 57, 2035–2059. https://doi.org/10.1007/s00603-023-03669-6.

12. Zafar, S., Hedayat, A., and Moradian, O. (2024). Stress Dependency of Brittle Creep in Granite: Insights into Source Mechanisms and Parameters. Rock Mech Rock Eng. https://doi.org/10.1007/s00603-024-04097-w

13. Imani, M., Walton, G., Moradian, O., Hedayat, A. (2024). Temporal and Spatial Evolution of Non-Elastic Strain Accumulation in Stanstead Granite During Brittle Creep. Rock Mech Rock Eng. https://doi.org/10.1007/s00603-024-04170-4.

Conference Proceedings

1. Imani, M, Hedayat, A, and G Walton. "Characterization and Monitoring of Damage Evolution in Brittle Rock During Primary, Secondary, and Tertiary Creep Phases." Paper presented at the 58th U.S. Rock Mechanics/Geomechanics Symposium, Golden, Colorado, USA, June 2024. doi: https://doi.org/10.56952/ARMA-2024-0617.

2. Zafar, S., Hedayat, A., and O. Moradian. "Time-Dependent Fracturing in Granite Under Uniaxial Compression." Paper presented at the 58th U.S. Rock Mechanics/Geomechanics Symposium, Golden, Colorado, USA, June 2024. doi: https://doi.org/10.56952/ARMA-2024-0786.

3. Butt, Awais, Hedayat, Ahmadreza, and Omid Moradian. "Seismic Investigation of Monotonic and Constant Pressure Hydraulic Fracturing Schemes in Granite." Paper presented at the 58th U.S. Rock Mechanics/Geomechanics Symposium, Golden, Colorado, USA, June 2024. doi: https://doi.org/10.56952/ARMA-2024-0618.

4. Imani, Mehrdad, Walton, Gabriel, Moradian, Omid, and Ahmadreza Hedayat. "Monitoring of Primary and Secondary Creep in Granite Using Ultrasonic Monitoring and Digital Image Correlation." Paper presented at the 57th U.S. Rock Mechanics/Geomechanics Symposium, Atlanta, Georgia, USA, June 2023. doi: https://doi.org/10.56952/ARMA-2023-0337.

5. Butt, Awais, Hedayat, Ahmadreza, and Omid Moradian. "Energy Budgeting of Laboratory Hydraulic Fracturing in Granite with Different Viscosity Injection Fluids." Paper presented at the 57th U.S. Rock Mechanics/Geomechanics Symposium, Atlanta, Georgia, USA, June 2023. doi: https://doi.org/10.56952/ARMA-2023-0751.

6. Zafar, Sana, Hedayat, Ahmadreza, Li, Bing Q., and Omid Moradian. "Brittle Creep and Associated Acoustic Emissions in Granite Under Unconfined Compression." Paper presented at the 57th U.S. Rock Mechanics/Geomechanics Symposium, Atlanta, Georgia, USA, June 2023. doi: https://doi.org/10.56952/ARMA-2023-0781.

7. Butt, Awais, Hedayat, Ahmadreza, and Omid Moradian. "Dry and Fluid Permeated Hydraulic Fractures and Their Geophysical Signatures in Granitic Rocks." Paper

presented at the 56th U.S. Rock Mechanics/Geomechanics Symposium, Santa Fe, New Mexico, USA, June 2022. doi: https://doi.org/10.56952/ARMA-2022-0406.

8. Zafar, Sana, Hedayat, Ahmadreza, and Omid Moradian. "Energy Partitioning During Fracturing in Granite Under Stress Relaxation." Paper presented at the 56th U.S. Rock Mechanics/Geomechanics Symposium, Santa Fe, New Mexico, USA, June 2022. doi: https://doi.org/10.56952/ARMA-2022-0548.

9. Butt, Awais, Hedayat, Ahmadreza, and Omid Moradian. "Acoustic Emission Source Mechanisms Evaluation of Hydraulically Induced Fractures in Brittle Rocks." Paper presented at the 55th U.S. Rock Mechanics/Geomechanics Symposium, Virtual, June 2021.

10. Butt, Awais, Hedayat, Ahmadreza, Tudisco, Erika, and Hamid Roshan. "Evaluation of Progressive Damage in Barre Granite using Ultrasonic Velocity Tomography and Digital Image Correlation." Paper presented at the 54th U.S. Rock Mechanics/Geomechanics Symposium, physical event cancelled, June 2020.

11. Butt, Awais, Fragomeni, Cara, Hedayat, Ahmadreza, and Erika Tudisco. "Applicability of Ultrasonic Tomographic Technique for Progressive Damage Evaluation in Prismatic Rock Specimen." Paper presented at the 53rd U.S. Rock Mechanics/Geomechanics Symposium, New York City, New York, June 2019.

12. Zafar, Sana, Hedayat, Ahmadreza, and Omid Moradian. "Laboratory Investigation of Stress Relaxation in Brittle Rocks Using Acoustic Emission and Digital Image Correlation." Paper presented at the 55th U.S. Rock Mechanics/Geomechanics Symposium, Virtual, June 2021.

13. Zafar, Sana, Hedayat, Ahmadreza, and Omid Moradian. "Acoustic Emission Monitoring of Progressive Damage in Prismatic Barre Granite Rocks with an Existing Flaw." Paper presented at the 54th U.S. Rock Mechanics/Geomechanics Symposium, physical event cancelled, June 2020.

14. Zafar, S., Hedayat, A., and Moradian, O. (2020). Evaluation of Crack Initiation and Damage in Intact Barre Granite Rocks Using Acoustic Emission. Proceedings of the Geo-Congress 2020 conference, February 25-28, 2020, Minneapolis, Minnesota.